Supporting Information

The dynamic evaporation process of deep eutectic solvent $LiTf_2N$:N-methylacetamide at ambient temperature

Yu Chen[*,‡,a], Dongkun Yu[‡,b], Li Fu [a], Meng Wang [a], Dongran Feng [a], Yingze Yang [a], Xiaomeng Xue [a], Jinfang Wang, [b] Tiancheng Mu[*, b]

[a] Department of Chemistry and Material Science, Langfang Normal University, Langfang 065000, Hebei, P.R. China. E-mail: yuchen@iccas.ac.cn; Phone: +86-0316-2188211; Fax: +86-0316-2112462. Zip: 065000.
[b] Department of Chemistry, Renmin University of China, Beijing 100872, P.R. China. E-mail: tcmu@ruc.edu.cn; Phone: +86-010-62514925; Fax: +86-010-62516444. Zip: 100872.

Contents

Cautions to IR measurement.

Pure potassium bromide (KBr) pellet was used as the substrate coated with DES for FT-IR measurement. However, during the volatilization process of $LiTf_2N$:NMA, the absorption of water from air by KBr might affect the experimental results. To exclude or minimize the effect of KBr hygroscopicity, we exposed KBr pellet overnight to the atmosphere. Figure 1a shows that the IR spectra of KBr pellet keep almost unchanged as a function of time in 295 min. Therefore, the effect of the water in KBr on the volatilization of $LiTf_2N$:NMA can be ignored

Interaction between $LiTf_2N$ and NMA.

The charge distribution of $LiTf_2N$ is: Li (+0.549), N (-0.964), O (-0.514, -0.498, -0.497, -0.445). The charge distribution of NMA is: NH (+0.5330), O (-0.506) N (-0.354). It implies that O in NMA (with the lowest negative charge -0.506) tends to coordinate with Li cation in $LiTf_2N$ (with the highest positive charge +0.549). H in NMA (+0.533) also tends to form intermolecular H-bonds with O of NMA (-0.506). However, the more negative charge of O in $LiTf_2N$ (-0.514, -0.498, -0.497, -0.445) provides a high possibility to form stronger H-bonds between NMA and $LiTf_2N$, hence $LiTf_2N$:NMA (mole ration 1:4) has extremely low melting point (-72 ^oC).[1] Similarly, H in NMA (+0.533) tends to form H-bonds with O in $LiTf_2N$ (-0.514). Although the N in $LiTf_2N$ (-0.964) is more negative than O (-0.506) in NMA, it can not prevent the stronger coordinating interaction of O in NMA around the Li cation in $LiTf_2N$. The attraction between O in $LiTf_2N$ and H in NMA can also enhance the coordination between O in NMA around the Li cation.[2]

The interaction can also be corroborated by the HOMO-LUMO energy (Scheme 1). The HOMO area of $LiTf_2N$ mainly exists around the atoms of O and N. The LUMO1 area of NMA concentrates around C atom and LUMO2 area of NMA is primarily dispersed around H(-N). Owing to the inertness of C atom in NMA to form H-bond, H(-N) of NMA in LUMO2 energy level tends to form H-bond with O or N of $LiTf_2N$. HOMO of $LiTf_2N$ and LUMO of NMA also show the possible interaction between Tf_2N and NMA. Li cation and O atom mainly occupy the HOMO area of $LiTf_2N$ and the LUMO1 area of NMA, respectively. It means the O atom in NMA mainly coordinates with Li cation. The 1:4 mole ratio of $LiTf_2N$ to NMA provides sufficient O atoms from NMA to coordinate with Li cation to form DES with the lowest melting point of -72 ^oC.[1]

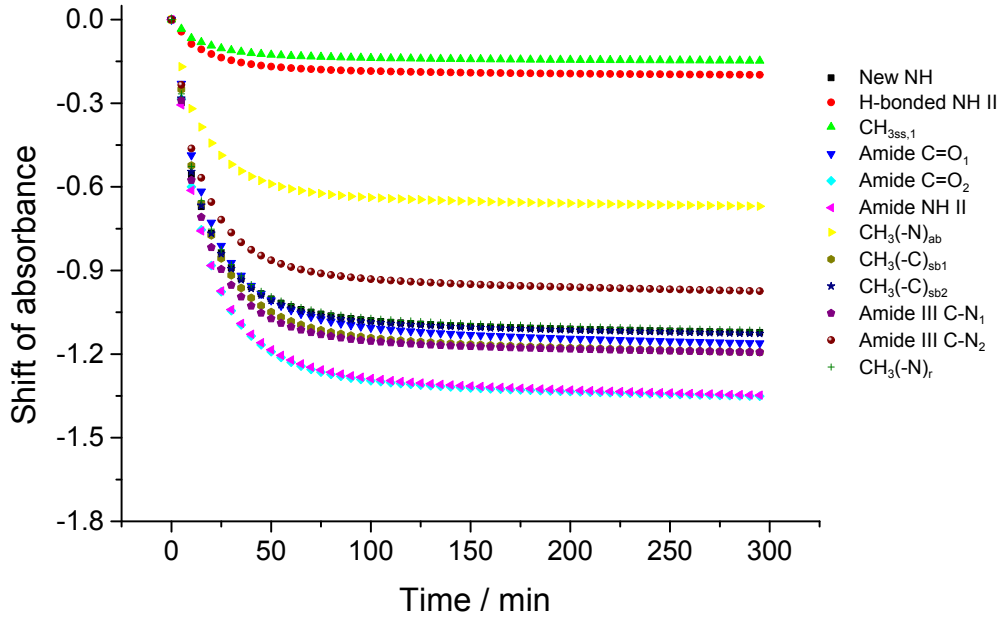

Figure S1. Shift of intensity for difference IR peak absorbance of $LiTf_2N$:NMA as a function of time.

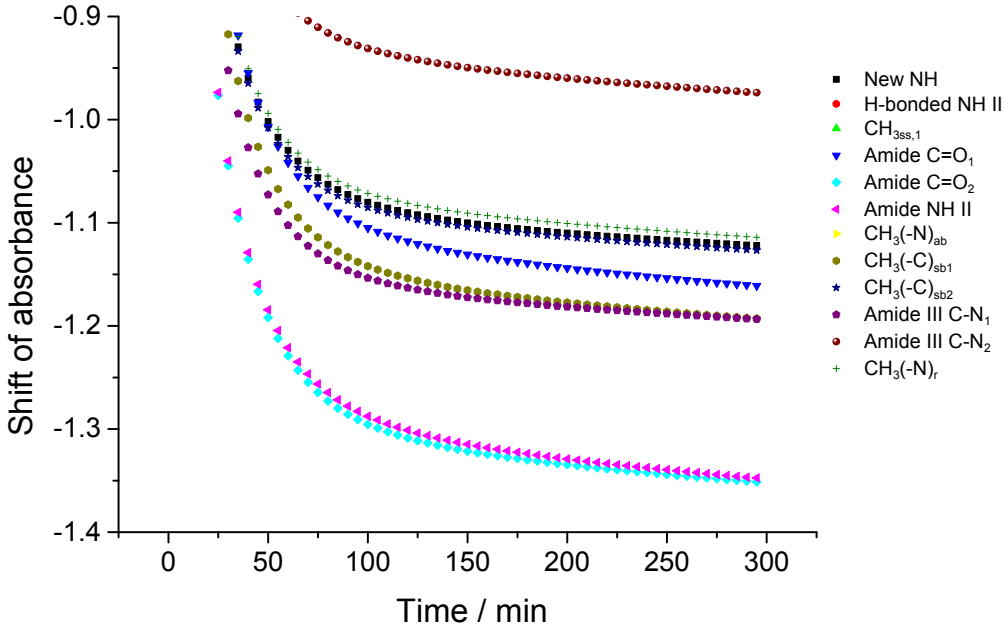

Figure S2. Expanded shift of intensity for difference IR peak absorbance of $LiTf_2N$:NMA as a function of time.

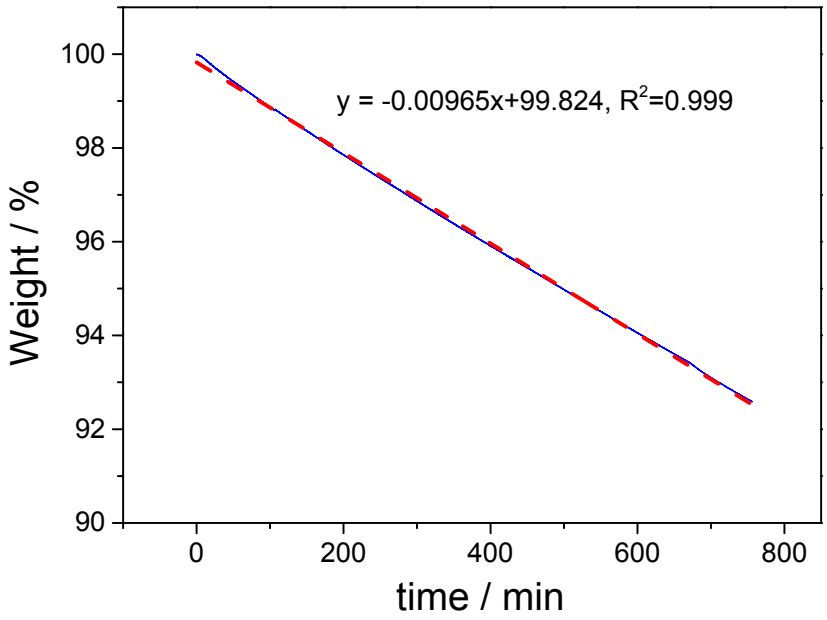

Figure S3. Weight change of DESs $LiTf_2N$:NMA (5.00600 mg) as a function of time at 20 °C in TGA. The blue solid line is the measured data. The red dash line is the fitted curve.

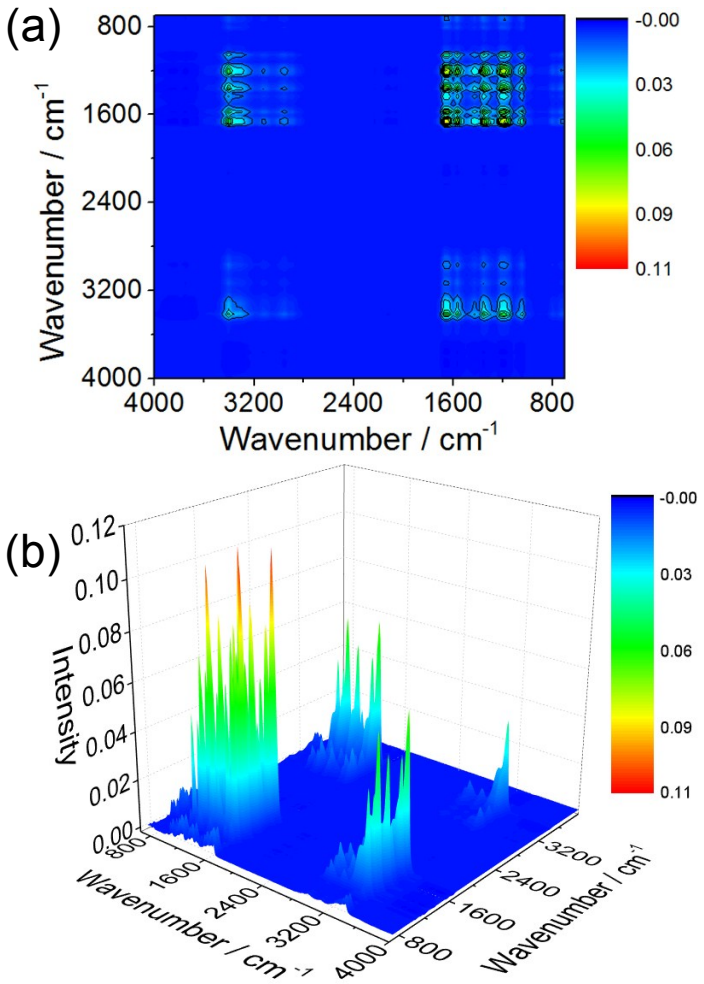

Figure S4. Synchronous G-2DCOS spectra for DESs $LiTf_2N$:NMA perturbated with time in the planar (a) and stereoscopic (b) mode.

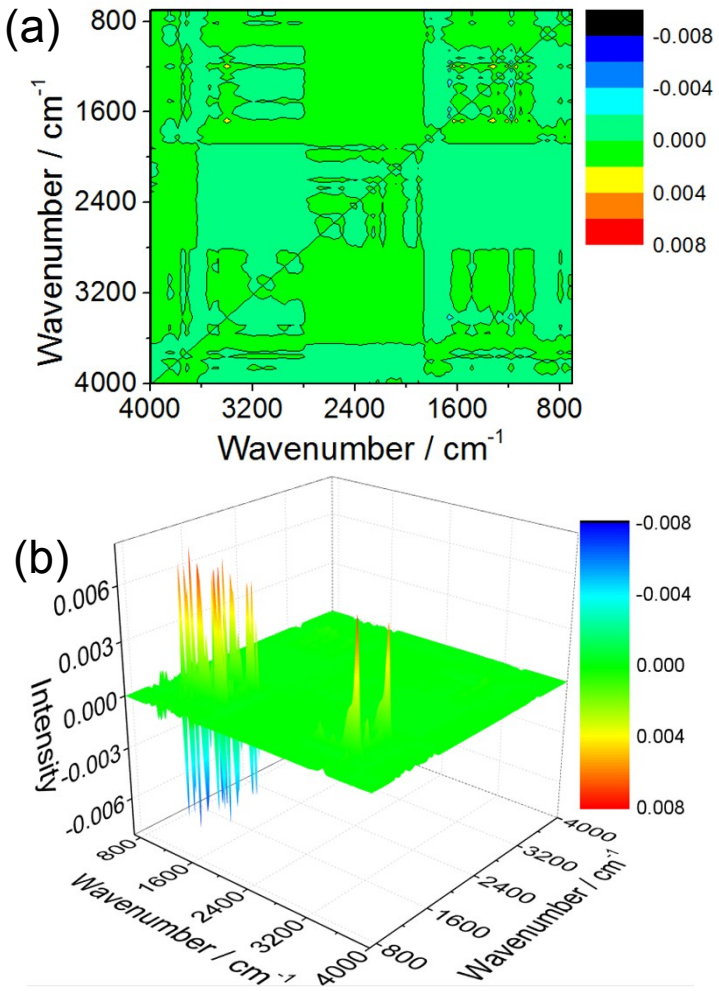

Figure S5. Asynchronous G-2DCOS spectra for DESs $LiTf_2N$:NMA perturbated with time in the planar (a) and stereoscopic (b) mode.

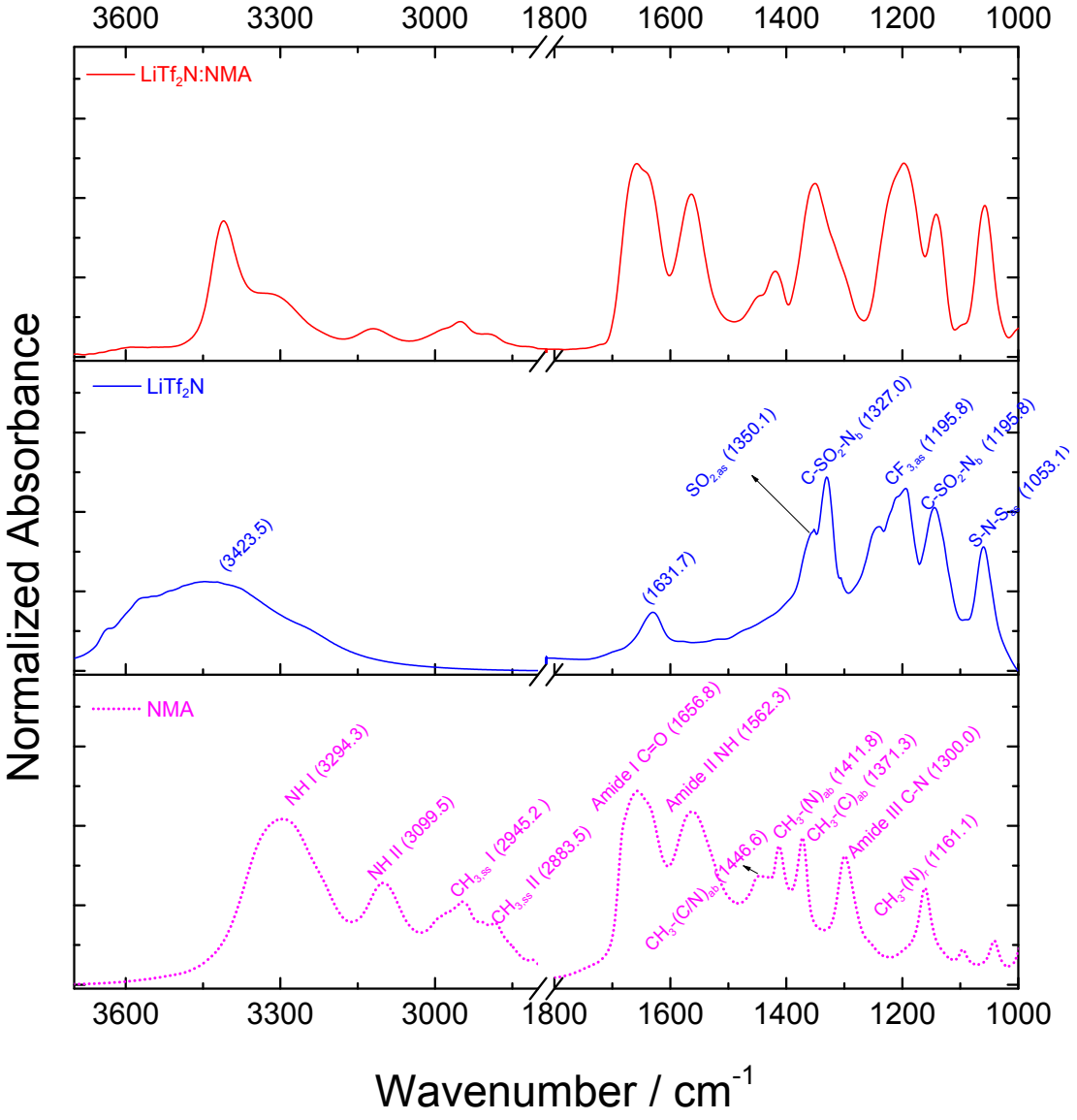

Figure S6. IR assignment for the reactants of DES: NMA and $LiTf_2N$.

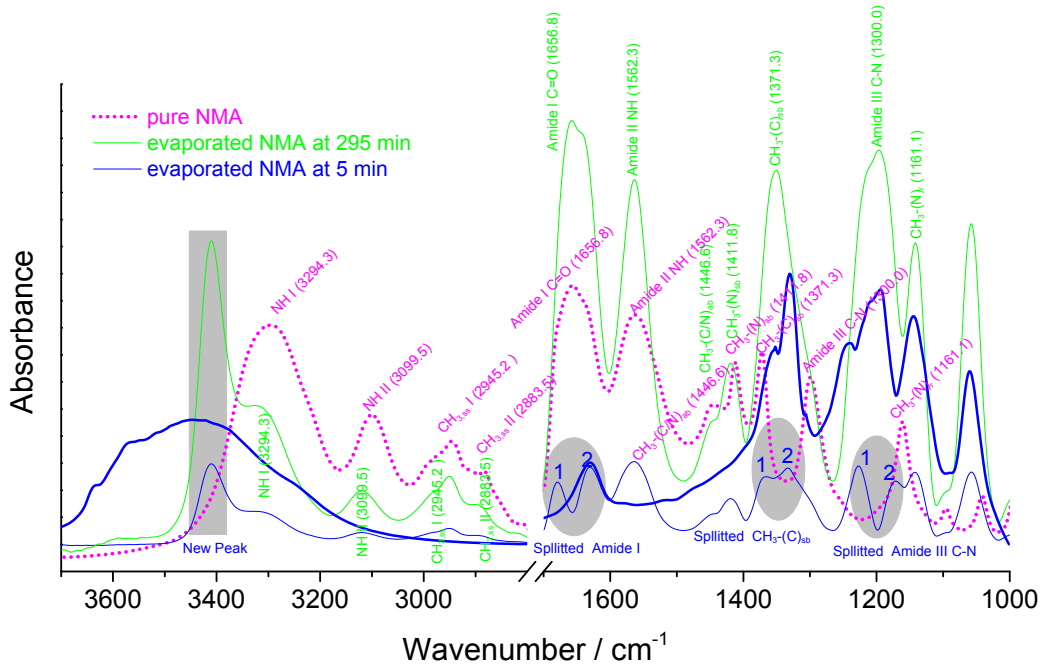

Figure S7. IR assignment for pure NMA and the evaporated NMA from DES $LiTf_2N$:NMA (1:4). The grey area is the peak with extensive alternation after evaporation. IR of the evaporated NMA is derived by the absolute value of difference spectra between IR spectrum of $LiTf_2N$:NMA at any time and at 0 min.

Table S1. Comparison the interaction energy of NMA/NMA and $LiTf_2N$/NMA via Gaussian calculation by B3LYP/6-31++g(d,p) method.

Interaction Energy / KJ/mol	$LiTf_2N$/NMA (1:1)	NMA/NMA (1:1)
ΔU	-149.7	-24.9
ΔH	-152.1	-27.3
ΔG	-110.7	9.9

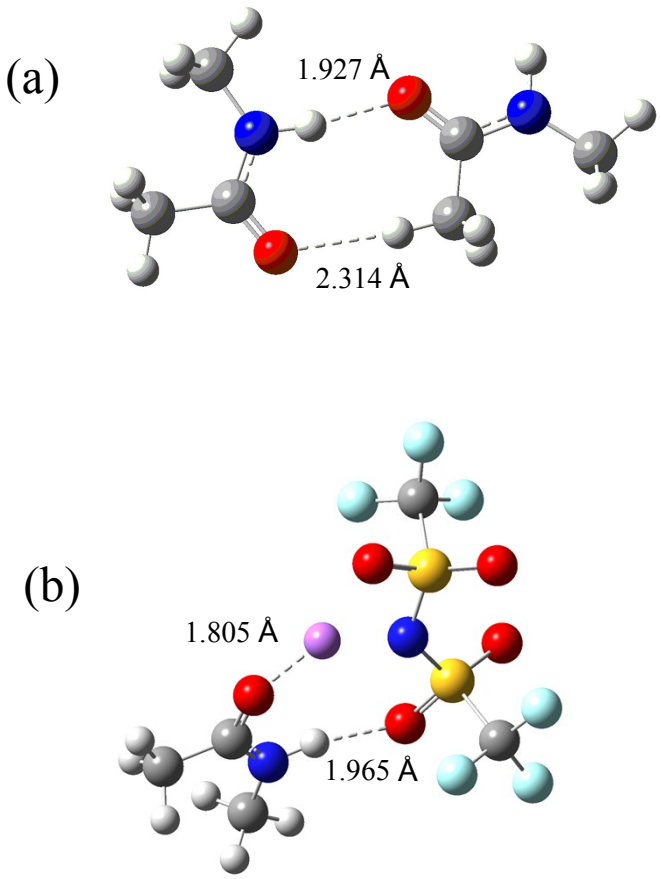

Figure S8. Optimal structure and intermolecular bond length of NMA/NMA (a) and $LiTf_2N$/NMA. O (red), N (blue), S (yellow), Li (pink), F (virid), C (grey), H (light grey) via Gaussian calculation by B3LYP/6-31++g(d,p) method.

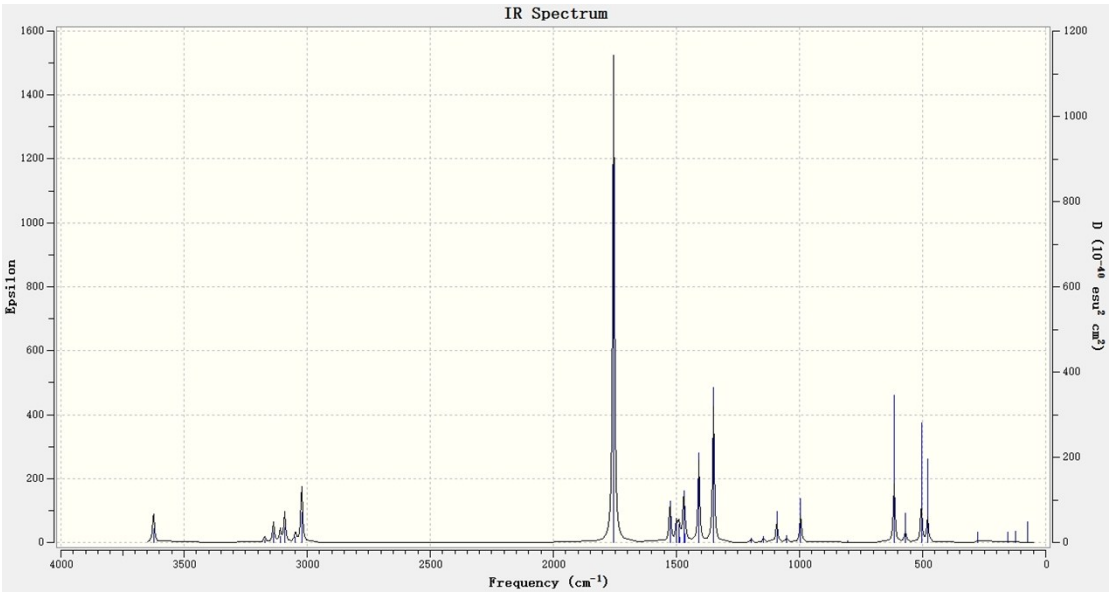

Figure S9. Simulated IR spectra of NMA via Gaussian calculation by B3LYP/6-31++g(d,p) method.

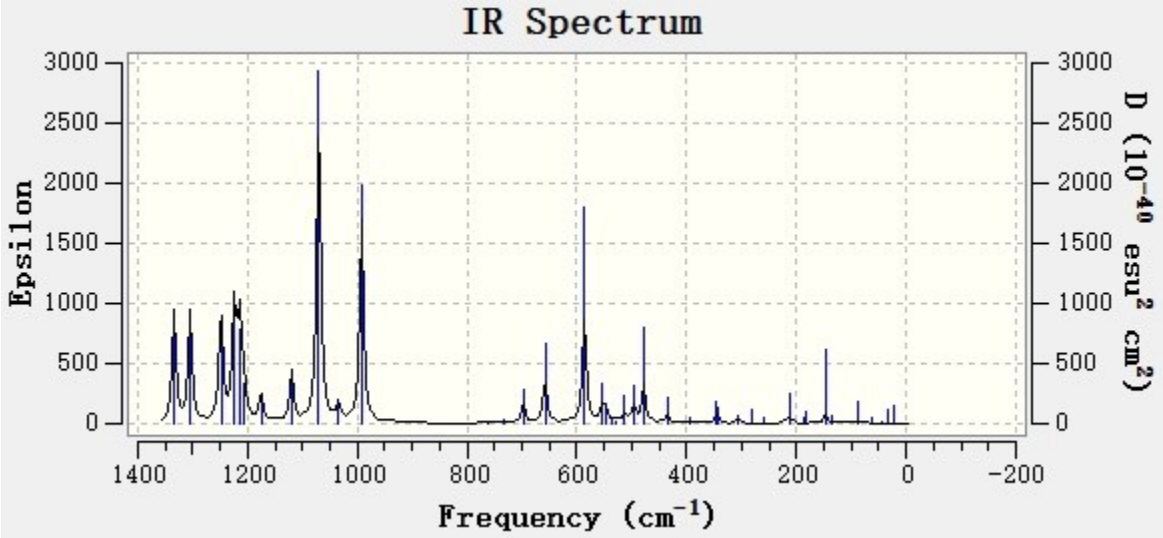

Figure S10. Simulated IR spectra of $LiTf_2N$ via Gaussian calculation by B3LYP/6-31++g(d,p) method.

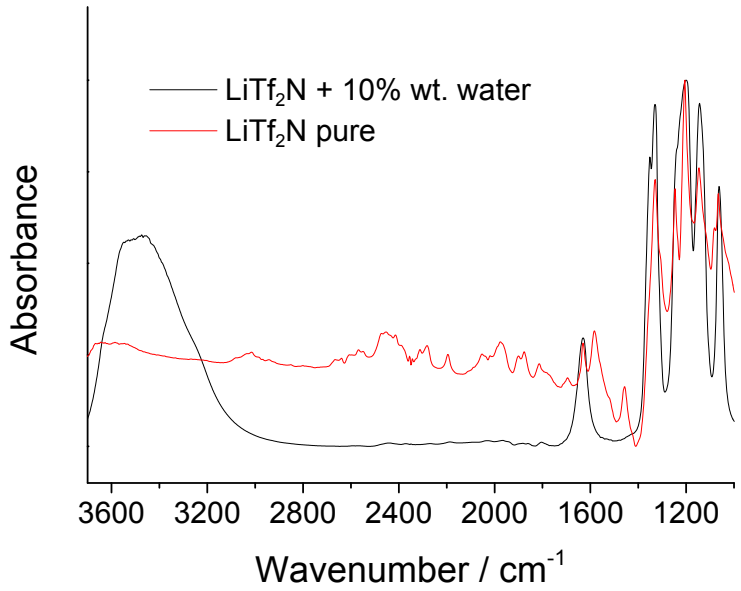

Figure S11. IR spectra of pure $LiTf_2N$ and $LiTf_2N$+10% wt. water on the surface of KBr pellet.

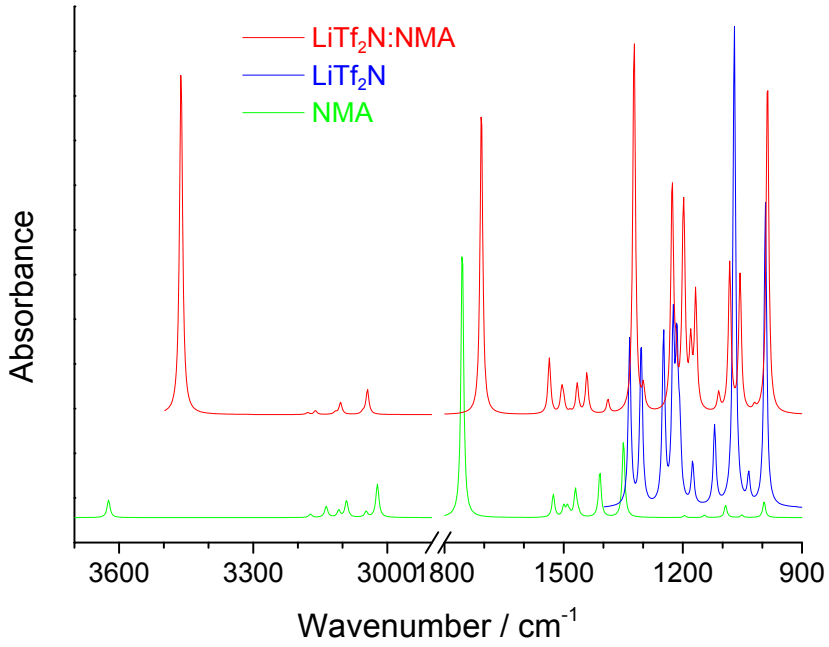

Figure S12. Comparison of the simulated IR spectra for NMA, $LiTf_2N$ and $LiTf_2N$:NMA via Gaussian calculation by B3LYP/6-31++g(d,p) method.

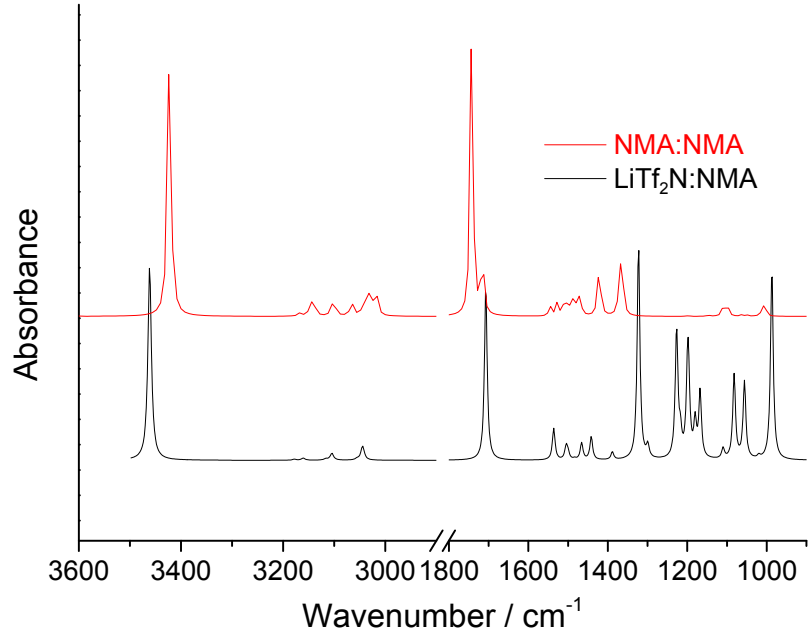

Figure S13. Comparison of the simulated IR spectra for NMA:NMA and $LiTf_2N$:NMA via Gaussian calculation by B3LYP/6-31++g(d,p) method.

Table S2. Comparison of simulated IR spectra for NMA, NMA:NMA, $LiTf_2N$ and $LiTf_2N$:NMA via Gaussian calculation by B3LYP/6-31++g(d,p) method.

$LiTf_2N$:NMA			NMA:NMA			NMA			$LiTf_2N$		
Mode #	Freq/ cm^{-1}	Intensity	Mode #	Freq/ cm^{-1}	Intensity	Mode #	Freq / cm^{-1}	Intensity	Mode #	Freq/ cm^{-1}	Intensity
1	13.15	0.4489	1	24.00	2.7697	1	75.35	0.8759	1	22.17	0.8340
2	14.39	0.4716	2	32.84	10.0544	2	123.38	0.7969	2	34.87	0.9515
3	27.68	0.0141	3	43.65	0.1520	3	153.58	0.9422	3	42.67	0.1650
4	34.12	0.3962	4	66.97	0.2822	4	277.45	1.6554	4	62.04	0.8881
5	39.25	0.0622	5	71.68	0.6984	5	479.74	23.5122	5	88.71	3.8954
6	46.88	0.3424	6	77.33	5.3690	6	505.23	35.5831	6	136.00	2.3160
7	56.86	0.7176	7	90.21	0.5234	7	569.59	9.7093	7	146.35	22.8772
8	70.45	0.3745	8	109.96	3.9047	8	615.63	53.4088	8	182.55	4.3168
9	72.93	6.0523	9	125.76	0.0117	9	805.19	0.6918	9	187.33	2.2787
10	95.43	2.7950	10	148.10	1.6183	10	995.41	25.6670	10	212.46	13.3799
11	103.68	1.0513	11	174.00	0.9744	11	1051.60	4.0932	11	253.36	0.3637
12	121.73	0.8610	12	183.39	0.0441	12	1092.42	19.8704	12	260.17	3.6185
13	141.73	7.3355	13	280.60	2.3806	13	1145.59	3.9990	13	281.01	8.3676
14	147.34	1.7203	14	294.16	7.6134	14	1195.68	3.2698	14	306.62	1.9205
15	173.53	16.2307	15	495.62	28.0453	15	1349.42	123.3231	15	307.03	5.0613
16	193.07	1.7623	16	496.46	20.7302	16	1408.88	74.0220	16	342.40	11.4255
17	198.31	5.2794	17	514.84	28.6680	17	1463.35	7.4602	17	345.73	16.1377
18	202.00	4.2650	18	573.73	11.4859	18	1470.25	44.5541	18	392.26	4.4858
19	231.18	14.5005	19	577.98	0.9317	19	1485.00	4.4915	19	434.56	23.1539
20	253.03	0.6282	20	580.99	24.7446	20	1490.77	15.6635	20	478.48	95.1102
21	274.36	6.4678	21	626.04	54.0551	21	1499.87	17.2906	21	495.97	38.8402
22	280.14	4.2273	22	792.30	69.0425	22	1526.08	37.0470	22	512.78	30.1367
23	289.12	26.7374	23	811.61	1.6512	23	1755.14	441.7294	23	528.27	1.7420
24	300.61	1.9580	24	815.69	0.2864	24	3022.10	54.2240	24	536.84	3.6586
25	306.39	10.2427	25	1003.11	19.1355	25	3047.38	9.1511	25	546.90	23.2032
26	337.72	0.4173	26	1010.04	28.1448	26	3091.20	27.3037	26	553.16	45.0943
27	342.57	2.7383	27	1049.50	3.3056	27	3108.74	11.3589	27	586.30	265.3350
28	376.18	3.1146	28	1062.94	4.1659	28	3136.67	18.1419	28	658.08	110.4924
29	391.46	2.3238	29	1098.85	31.2896	29	3172.18	5.5294	29	697.56	50.2632
30	487.10	9.5398	30	1109.06	30.7901	30	3623.76	28.5197	30	731.56	6.5739
31	504.64	58.5183	31	1145.87	0.1566	31			31	761.10	0.5318
32	514.86	0.1360	32	1147.28	3.4999	32			32	992.22	492.9538
33	536.28	0.4214	33	1195.92	0.4046	33			33	1034.26	45.8531
34	541.65	1.2202	34	1197.94	1.4361	34			34	1070.44	785.8605
35	555.12	39.8130	35	1364.49	155.7065	35			35	1120.03	127.8564
36	560.26	17.4554	36	1370.12	78.4193	36			36	1175.35	68.5022
37	573.37	19.6768	37	1419.68	79.7545	37			37	1207.70	100.6319

38	578.44	1.1453	38	1423.86	72.6856	38		38	1214.96	237.5610
39	594.38	340.2436	39	1464.62	5.2778	39		39	1224.43	278.6757
40	614.90	29.8921	40	1470.31	28.4930	40		40	1248.55	279.1375
41	664.44	159.8127	41	1475.58	49.8159	41		41	1304.95	266.6539
42	718.32	106.1621	42	1484.47	1.7233	42		42	1334.03	269.3551
43	750.24	0.9865	43	1487.94	34.6995	43				
44	769.34	34.0835	44	1490.74	4.6243	44				
45	779.40	63.4764	45	1497.39	11.7537	45				
46	843.33	13.6662	46	1502.30	18.3091	46				
47	986.98	554.3010	47	1508.39	23.7660	47				
48	1019.80	8.1429	48	1511.20	12.9509	48				
49	1056.02	218.0471	49	1527.17	36.8935	49				
50	1058.73	4.3331	50	1545.24	27.3247	50				
51	1082.07	240.7269	51	1715.46	184.6088	51				
52	1109.84	29.5780	52	1742.76	834.3587	52				
53	1144.64	0.1206	53	3018.75	76.7688	53				
54	1167.67	188.3186	54	3030.52	44.4462	54				
55	1180.21	99.3538	55	3036.68	44.3877	55				
56	1194.19	4.4719	56	3044.58	12.8856	56				
57	1196.51	140.8154	57	3065.74	37.4358	57				
58	1199.14	223.9921	58	3099.44	26.9076	58				
59	1217.27	60.3896	59	3103.15	7.5905	59				
60	1226.87	371.0005	60	3104.24	14.9578	60				
61	1299.38	35.7166	61	3138.74	15.5627	61				
62	1322.66	613.8311	62	3140.28	15.5774	62				
63	1388.63	22.2187	63	3145.94	32.9298	63				
64	1441.62	65.7506	64	3168.29	7.7970	64				
65	1465.89	48.3625	65	3422.87	747.0702	65				
66	1484.01	3.7421	66	3621.62	28.7697	66				
67	1499.51	14.0844				67				
68	1503.51	21.1055				68				
69	1505.54	21.9580				69				
70	1536.11	90.7356				70				
71	1707.12	504.9029				71				
72	3044.43	40.4596				72				
73	3055.06	3.5215				73				
74	3104.60	19.6976				74				
75	3116.44	3.8702				75				
76	3160.71	6.2175				76				
77	3178.26	3.0687				77				
78	3461.39	562.2504				78				

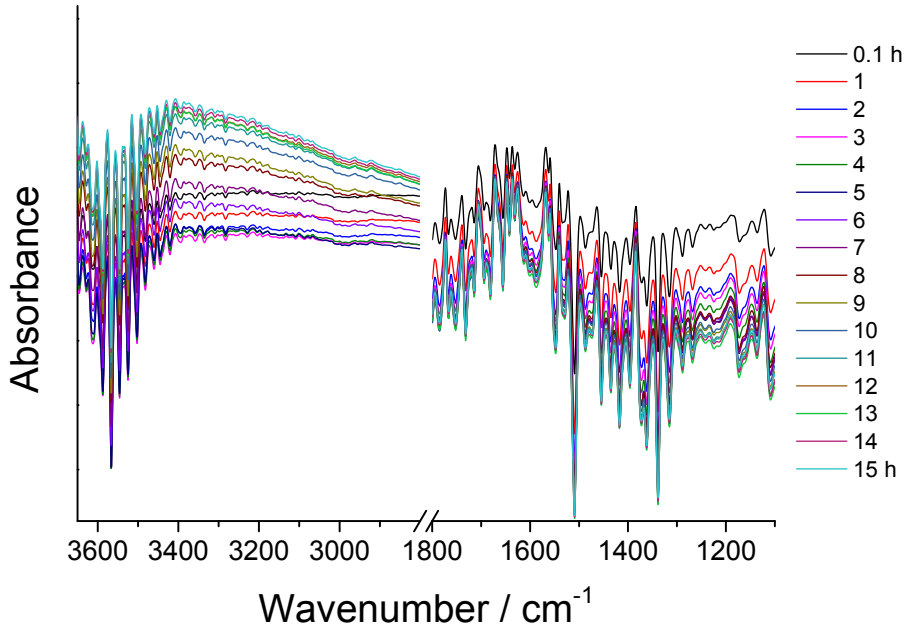

Figure S14. TG-IR spectra of $LiTf_2N$:NMA (1:4 mol ratio, 12.2700 mg) at 27 °C at N_2 atmosphere in alumina pan for 15 h measured by the couple of Mettler Toledo TGA/DSC3+ with Thermo Scientific Nicolet iS50 FT-IR.

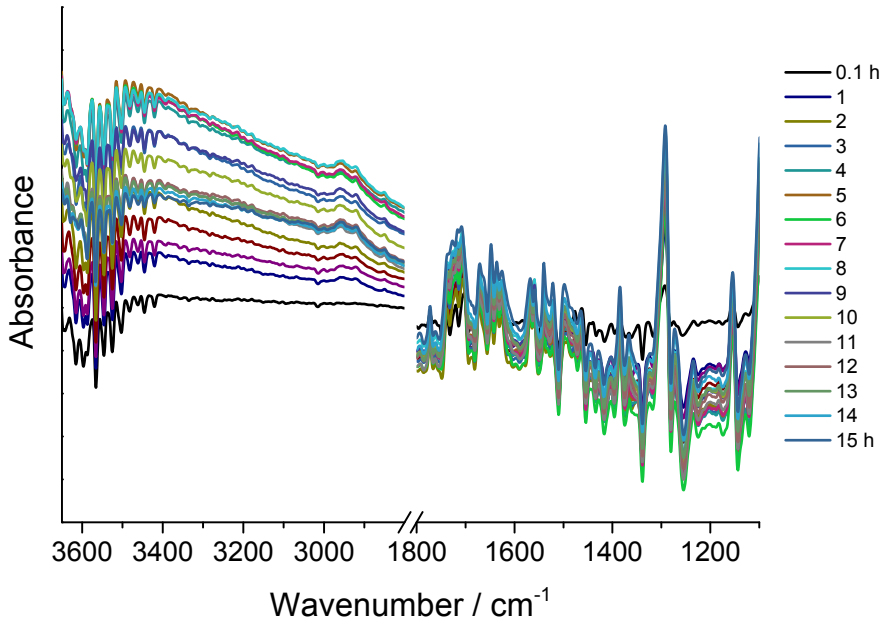

Figure S15. TG-IR spectra of pure NMA (15.4670 mg) at 27 °C at N_2 atmosphere in alumina pan for 15 h measured by the couple of Mettler Toledo TGA/DSC3+ with Thermo Scientific Nicolet iS50 FT-IR.

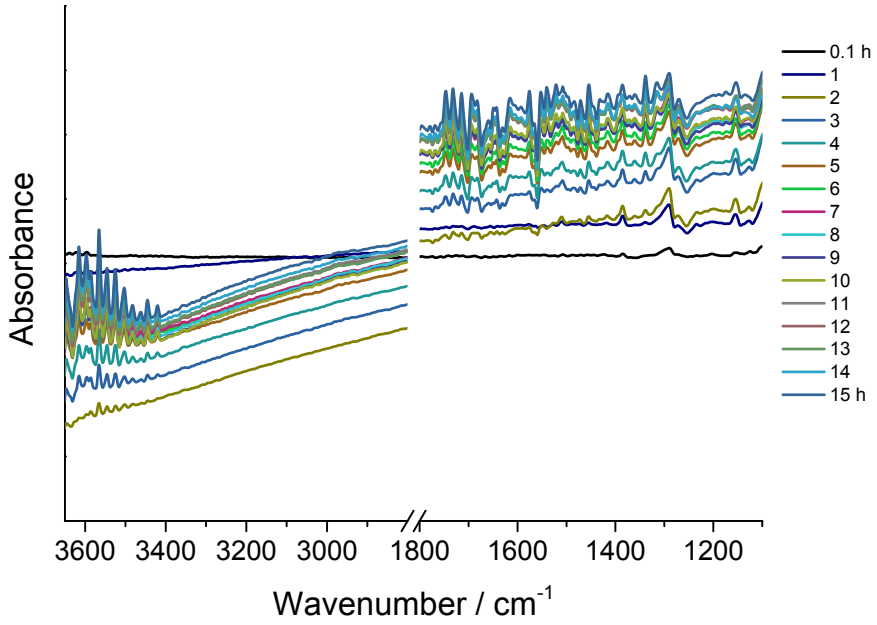

Figure S16. TG-IR spectra of pure water (19.3900 mg) at 27 °C at N_2 atmosphere in alumina pan for 15 h measured by the couple of Mettler Toledo TGA/DSC3+ with Thermo Scientific Nicolet iS50 FT-IR.

Table S3. Cartesian coordinates of all the optimized species by the Gaussian calculation (i.e., output file) for NMA:NMA.

C	-0.64935600	1.10785700	0.53231500
O	-1.04668200	1.48391600	1.64200700
C	-1.07019800	-0.23604800	-0.04239200
H	-0.20157900	-0.87707400	-0.23125600
H	-1.72870500	-0.72530900	0.67495100
H	-1.59963500	-0.11332600	-0.99407000
N	0.17922100	1.87120500	-0.22635300
H	0.45384000	2.77298500	0.17078400
C	0.70199900	1.52856900	-1.53869400
H	-0.09320300	1.39608200	-2.28313100
H	1.33974600	2.34987000	-1.87095500
H	1.31013700	0.61552000	-1.51948600
C	0.87127800	5.09202800	1.74736800
O	1.13224500	4.49922700	0.69208100
C	-0.10262600	4.55162500	2.77209300
H	0.35892700	4.49982700	3.76440400
H	-0.97504900	5.21115800	2.85168600
H	-0.43504800	3.55565500	2.47166700
N	1.46173100	6.29196000	2.01591600
H	2.12673600	6.59196900	1.31512700
C	1.31999000	7.08461700	3.22895500
H	1.83189700	6.63138100	4.08722200
H	1.75661400	8.06961000	3.05206700
H	0.26682900	7.22675100	3.48739600

1 2 2.0 3 1.0 7 1.5
2
3 4 1.0 5 1.0 6 1.0
4
5
6
7 8 1.0 9 1.0
8
9 10 1.0 11 1.0 12 1.0
10
11
12
13 14 2.0 15 1.0 19 1.5
14
15 16 1.0 17 1.0 18 1.0
16

17
18
19 20 1.0 21 1.0
20
21 22 1.0 23 1.0 24 1.0
22
23
24

Table S4. Cartesian coordinates of all the optimized species by the Gaussian calculation (i.e., output file) for $LiTf_2N$:NMA.

N	-0.57718800	-0.70281000	-0.52794500
O	-2.77973100	-0.17960200	-1.32444500
O	1.83813400	0.27928400	-0.71842000
O	1.35295100	-1.98714300	0.33930700
O	-1.24959200	1.83308400	-0.93617100
S	0.95551500	-0.60119600	0.03771000
S	-1.42308000	0.44127800	-1.32484400
C	-0.89620900	0.32909900	-3.13991600
C	0.76499000	0.18567800	1.74691900
F	-0.09235100	-0.53732900	2.48862600
F	1.95814900	0.19475600	2.35155300
F	0.30737000	1.43364400	1.64906100
F	-0.96792600	-0.94608000	-3.55209100
F	0.34758600	0.77369200	-3.30128500
F	-1.73560700	1.07143900	-3.86896000
Li	-2.24690800	-1.86019400	-0.41219100
C	-1.61402200	-4.53802800	0.55236400
O	-2.30951200	-3.57061000	0.15954400
C	-2.26336900	-5.87141700	0.83929900
H	-2.14550100	-6.14148900	1.89435900
H	-3.32434100	-5.80359000	0.60245400
H	-1.80668900	-6.66857500	0.24356300
N	-0.29163700	-4.42187800	0.73155400
H	0.12959100	-3.51221700	0.53577900
C	0.61127500	-5.47764500	1.18008000
H	0.65423100	-6.30562400	0.46446100
H	1.60888200	-5.04613400	1.26618300
H	0.31919500	-5.86945500	2.15962100

1 6 1.0 7 1.0
2 7 2.0

3 6 2.0
4 6 2.0
5 7 2.0
6 9 1.0
7 8 1.0
8 13 1.0 14 1.0 15 1.0
9 10 1.0 11 1.0 12 1.0
10
11
12
13
14
15
16
17 18 2.0 19 1.0 23 1.5
18
19 20 1.0 21 1.0 22 1.0
20
21
22
23 24 1.0 25 1.0
24
25 26 1.0 27 1.0 28 1.0
26
27
28

Table S5. Cartesian coordinates of all the optimized species by the Gaussian calculation (i.e., output file) for $LiTf_2N$.

N	-0.27993200	-0.22443200	-0.35546200
O	-1.66313100	-1.35744500	-1.97000300
O	-1.25757400	1.88432200	0.81400900
O	1.25948300	1.53337300	0.79205900
O	-1.27403300	1.13854200	-2.39784500
S	-0.09633600	1.00207600	0.73336900
S	-0.79617000	-0.13482100	-1.88381600
C	0.73139400	-0.58429200	-2.89723200
C	-0.26033700	-0.18763200	2.20908800
F	0.83421400	-0.92301900	2.38546400
F	-0.53722500	0.48570700	3.31615000
F	-1.31049900	-1.07018700	1.98641600
F	1.23427100	-1.75162700	-2.47616300
F	1.65040700	0.37091600	-2.75646100
F	0.38564500	-0.69171500	-4.18239100
Li	-1.54109900	-1.73547800	-0.07733000

1 6 1.0 7 1.0
2 7 2.0
3 6 2.0
4 6 2.0
5 7 2.0
6 9 1.0
7 8 1.0
8 13 1.0 14 1.0 15 1.0
9 10 1.0 11 1.0 12 1.0
10
11
12
13
14
15
16

Table S6. Cartesian coordinates of all the optimized species by the Gaussian calculation (i.e., output file) for NMA.

C	0.44992900	0.27191700	0.53131900
O	1.05641800	-0.04156600	1.55318900
C	0.39648300	-0.63133600	-0.68924600
H	0.76225500	-0.11887400	-1.58574800
H	1.01768800	-1.50471200	-0.49289200
H	-0.62952800	-0.95948500	-0.89078200
N	-0.22949900	1.45909400	0.44886800
H	-0.12892000	2.04439500	1.26762000
C	-0.90012600	2.00674000	-0.72059500
H	-1.58404000	1.27679900	-1.16397000
H	-1.49397100	2.86849000	-0.40883000
H	-0.19613600	2.33960200	-1.49479400

1 2 2.0 3 1.0 7 1.5
2
3 4 1.0 5 1.0 6 1.0
4
5
6
7 8 1.0 9 1.0
8
9 10 1.0 11 1.0 12 1.0
10
11
12

References

(1) Boisset, A., Menne, S., Jacquemin, J., Balducci, A. & Anouti, M., Deep eutectic solvents based on N-methylacetamide and a lithium salt as suitable electrolytes for lithium-ion batteries. *Phys. Chem. Chem. Phys.* **2013**, 15, 20054-20063.

(2) Sim, L. N., Yahya, R. & Arof, A. K., Infrared studies of polyacrylonitrile-based polymer electrolytes incorporated with lithium bis(trifluoromethane)sulfonimide and urea as deep eutectic solvent. *Opt. Mater.* **2016**, 56, 140-144.